Pergamon

Scripta Metallurgica *et* Materialia, Vol. 33, Nos. 10/11, pp. 1831-1839, 1995
Elsevier Science Ltd

0956-716X/95 $9.50 + .00

0956-716X(95)00393-2

STRESS AND STRAIN IN MICRO- AND NANO-STRUCTURED INTERSTITIAL MAGNETS

R. Skomski
Physics Department, Trinity College, Dublin 2, Ireland

Hooke's law is used to calculate the elastic stress and strain in interstitial magnets. Emphasis is put on spherical and plate-like $Sm_2Fe_{17}N_x$ particles with continuous and discontinuous interstitial concentration profiles, hypothetical high-performance $Sm_2Fe_{17}N_{3-\delta}$/FeCo composites, and 'natural' multilayers such as $Nd_6Fe_{13}CuH_x$, where the recently discovered large anisotropic lattice expansion is shown to arise from the crystal structure.

Das Hookesche Gesetz wird benutzt, um elastische Spannungen und Dehnungen in Zwischengittermagneten zu berechnen. Hauptgegenstand der Untersuchung sind kugelförmige und flache $Sm_2Fe_{17}N_x$ Teilchen mit kontinuierlichen und diskontinuierlichen Zwischengitterkonzentrations-profilen, hypothetische $Sm_2Fe_{17}N_{3-\delta}$/FeCo Hochleistungskomposite und natürliche Vielfachschichten wie $Nd_6Fe_{13}CuH_x$, deren unlängst entdeckte große anisotrope Gitteraufweitung auf die Kristallstruktur zurückgeführt wird.

Introduction

The discovery [1] that nitrogen introduced from the gas phase drastically improves the permanent magnetic performance of Sm_2Fe_{17} has sparked the interest in interstitial permanent magnets [2-12]. Since then, interstitial modification using molecular nitrogen, ammonia, and hydrocarbon gases has been extended to other intermetallics to yield materials such as $R_2Fe_{17}Z_{3-\delta}$ and $R(Fe_{11}Ti)Z_{1-\delta}$ (Z = N, C) [3]. Besides, $R_2Fe_{17}C_x$ carbides with $x > 2$ are obtained by solid-solid interstitial modification using graphite [13], while the introduction of carbon directly from the melt leads to smaller carbon contents $x \leq 1.5$ [14]. Hydrogen has long been known as an interstitial in transition-metal-rich rare-earth intermetallics such as $LaNi_5$, Sm_2Fe_{17}, and $Nd_2Fe_{14}B$, but here the changes in magnetic properties are less pronounced [15-17].

A characteristical feature of interstitially modified crystals is the occurence of elastic stress and strain [2, 18-20]. Compared to the considerable interest in the magnetic and thermodynamic properties of the new materials [3-6, 8-10, 12], the elastic behaviour of the new interstitial nitrides and hydrides has attracted much less attention [2]. From the point of view of elastic properties, hydrogen and nitrogen in metals have a great deal in common. In particular, the long-range elastic strain in interstitially modified metals, which is responsible for the phase structure of the gas-metal systems [18-20], does not depend on the chemical nature of the interstitial atoms. On the other hand, strain-related phenomena such as the magnetic soft-core problem [2, 21] shape the processing behaviour of interstitial permanent magnets and justify a separate treatment of the ferromagnetic nitrides, carbides, and hydrides.

In this work we investigate elastic stress and strain in interstitially modified rare-earth transition-metal ferromagnets. In Section 2 we summarize how the permanent magnetic performance of iron-rich rare-earth intermetallics is improved upon interstitial modification. Section 3 is devoted to the quasi-equilibrium phase structure of $Sm_2Fe_{17}N_x$, while stress and strain profiles in homogeneously and inhomogeneously modified

$Sm_2Fe_{17}N_x$ particles are calculated in Section 4. The last section of this paper deals with artificial two-phase multilayers such as $Sm_2Fe_{17}N_{3-\delta}$/FeCo, whose permanent magnetic properties have been predicted to be better than those of any known single-phase material [22-24], and 'natural' multilayers such as $Nd_6Fe_{13}CuH_x$ [25].

Background

Single-Phase Materials

As shown by Coey and Sun [1], interstitial 2p atoms can be used to yield a considerable improvement of the permanent magnetic performance of iron-rich rare-earth intermetallics. In the case of $Sm_2Fe_{17}N_{3-\delta}$, where this improvement is most pronounced, the dramatic effect of the interstitial atoms is a large Curie-temperature increase, from 116 °C for Sm_2Fe_{17} to 476 °C for $Sm_2Fe_{17}N_{3-\delta}$ [3]. Furthermore, $Sm_2Fe_{17}N_{3-\delta}$ exhibits easy-axis anisotropy in contrast to the easy-plane behaviour of the parent compound Sm_2Fe_{17}, which is not suitable for permanent magnetic applications [1, 3].

Nitrogen and carbon in Sm_2Fe_{17} occupy the octahedral 9e interstices (Figures 1 and 2) in the rhombohedral Th_2Zn_{17} structure [11] [6], although there is some evidence that non-equilibrium gas-phase interstitial modification using ammonia yields an additional occupancy of the 3b site [6, 12]. Apart from the possibility of short-circuit diffusion along microcracks, the modification reaction consists in the thermally activated bulk diffusion of the interstitial atoms [2, 7, 12]. Due to the low diffusivity of nitrogen in Sm_2Fe_{17}, $E_a \approx 133$ kJ/mole and $D_o \approx 1$ mm^2/s [2, 7], finely-ground powder has to be used to conduct the reaction; typical reaction conditions are T = 400-500 °C, $p(N_2) = 1$ bar, and t = 5 h [12]. A consequence of the comparatively long reaction times are inhomogeneous nitrogen concentration profiles during, or even after, the quasi-equilibrium reaction [2, 7, 12]. Note that the true equilibrium of the system involves the disproportionation of the intermetallic lattice and the formation of SmN, so that disproportionation kinetics (iron diffusion) makes it impossible to utilize nitrogenation temperatures higher than about 550 °C [1-4]. The elastic stress and strain caused by these inhomogenities is one subject of this work.

The Curie-temperature increase upon nitrogenation is a direct consequence of the lattice expansion [1, 3], which is of order $\Delta V/V = 6\%$ for $Sm_2Fe_{17}N_{3-\delta}$. As discussed by Skomski and Coey [2], the inhomogeneous lattice expansion in partly nitrided grains leads to a Curie-temperature increase at the particle centre even if there is no nitrogen there. On the other hand, the change from easy-plane to easy-axis anisotropy originates from the short-ranged, i.e. screened, electrostatic crystal field created by the nitrogen atoms [10]. This means that the magnetocrystalline anisotropy reflects the local nitrogen concentration rather than the local volume expansion, and the absence of nitrogen at the centre of a partly nitrided grain destroys the coercivity of the whole grain [21].

Another reason for the interest in the elastic behaviour of $Sm_2Fe_{17}N_x$ magnets is the complicated processing of the nitrides. The realization of coercivity in permanent magnets consists in the removal of lattice inhomogenities, which are likely to act as nucleation centres for the formation of reversed magnetic domains [22-24]. This means that large stress and strain is likely to destroy coercivity by enhancing the disproportionation of the intermetallic lattice. On the other hand, the formation of microcracks upon interstitial modification using N_2, H_2, and/or NH_3 can be used to facilitate the milling of Sm_2Fe_{17} ingots.

Finally, the phase structure of the interstitial nitrides is determined by the elastic and structural properties of the lattice (see Section 3).

Two-Phase Materials

Recently it has been shown [22-24] that the potential permanent magnetic performance of nanostrucured two-phase multilayers such as $Sm_2Fe_{17}N_3$/FeCo is better than that of any other material. The actual production of these structures is an extremely demanding task, but a conceivable way of production is layer-by-layer nitro-

genation of hypothetical Sm_2Fe_{17}/FeCo multilayers. Due to the two-dimensional constraint imposed by the multilayer's substrat, the elastic energy upon nitrogenation increases, and we have to investigate whether the modification reaction remains sufficiently exothermic to assure thorough nitrogenation.

A similiar problem arises in the recently discovered 6:13:1 hydrides [25] such as $Nd_6Fe_{17}CuH_x$. Upon interstitial modification the magnetic structure of the tetragonal changes from antiferromagnetic ($\mu \leq 1\ \mu_B$/ formula unit) to ferromagnetic ($\mu \approx 32\ \mu_B$/formula unit). A possible explanation of this behaviour is tthat the hydrogenation of the lattice, whose unit cell is reminiscent of a multilayer consisting of rare-earth-rich and iron slabs, yields a preferential expansion of the rare-earth slabs. This mechanism, which is described in Section 5, could then modify the coupling between the iron slabs responsible for the moment formation.

Phase Structure of Interstitial Nitrides

A key question is whether $Sm_2Fe_{17}N_x$, prepared at typical reaction temperatures (400-500 °C), is a gas-solid solution or a two-phase mixture of nitrogen-poor α and nitrogen β phases [2]. Phase segregation is caused by the attractive elastic interaction between different interstitial atoms and occurs below a critical temperature T_c [18-20]. Pictorially speaking, interstitial atoms enlarge the size of neighbouring interstices whose occupancy is now energetically more favourable. Below T_c this tendency dominates, i.e. thermal activation is not able to destroy clusters of interstitial atoms. In the case of a clamped surface, however, the size of neighbouring interstices actually decreases, and the interaction is repulsive [19].

There is overwhelming evidence that nitrogenation using molecular nitrogen and subsequent quenching yield a gas-solid solution [2, 7, 12]. In particular, X-ray diffraction analysis shows a single set of X-ray diffraction peaks [7, 12], while two-phase nitrides would reveal themselves by a double-peak structure of the diffraction pattern [19]. There are only 3 nitrogen atoms per 2 + 17 = 19 metal atoms in $Sm_2Fe_{17}N_3$, as compared to nearly one interstitial atom per metal atom in PdH_x. This leads to a fairly weak elastic interaction and a low critical temperature, even if we bear in mind that the volume expansion per interstitial nitrogen atom, $\Delta v \approx 7$ Å^3 [12], is larger than that per hydrogen atom in metals, typically $\Delta v \approx 3$ Å^3. In fact, due to the low nitrogen diffusivity below about 400 °C it has been impossible so far to measure the critical temperature of $Sm_2Fe_{17}N_x$.

It is worthwhile mentioning that critical fluctuations of interstitial atoms near T_c [26, 27] obey the mean-field predictions of the Landau theory [18], since the exactness of the mean field predictions increases with the system's dimensionality and the range of interatomic interaction, i.e. the effective number of interacting neighbours. Elastic strain caused by a localized 'impurity' exhibits a long-range $1/R^3$ power-law decays, as opposed to the short-range ferromagnetic exchange interaction. Another consequence of the long-range character of the interaction is that microscopic properties such as interstitial diffusivity depend on the macroscopic shape of the sample [18, 19]. This is is reminiscent of the long-range magnetostatic interaction, which is observed as shape dependent demagnetization factor.

Partly Nitrided $Sm_2Fe_{17}N_x$ Particles

During nitrogenation, inhomogeneous concentration profiles cause mechanical stress and strain which, in turn, affect magnetization and Curie temperature. Let us apply the formalism used in [2] and start from Hooke's law for isotropic elastic media

$$\sigma_{ik} = \frac{E}{1+\nu}(\varepsilon_{ik} - \varepsilon^{\circ}_{ik}) + \frac{\nu E}{(1+\nu)(1-2\nu)}\delta_{ik}\,\mathrm{Tr}(\varepsilon_{ik} - \varepsilon^{\circ}_{ik}) \qquad (1)$$

where E and ν are Young's modulus and Poisson's ratio, respectively. Here $\varepsilon_{ik}^{\circ} = \varepsilon_0 \langle c(\mathbf{r})\rangle\, \delta_{ik}$ denotes the stress-free reference expansion. From $\Delta V/V \approx 6\%$ and the average equilibrium occupancy $\langle c(\mathbf{r})\rangle \approx 1$ [2, 7,

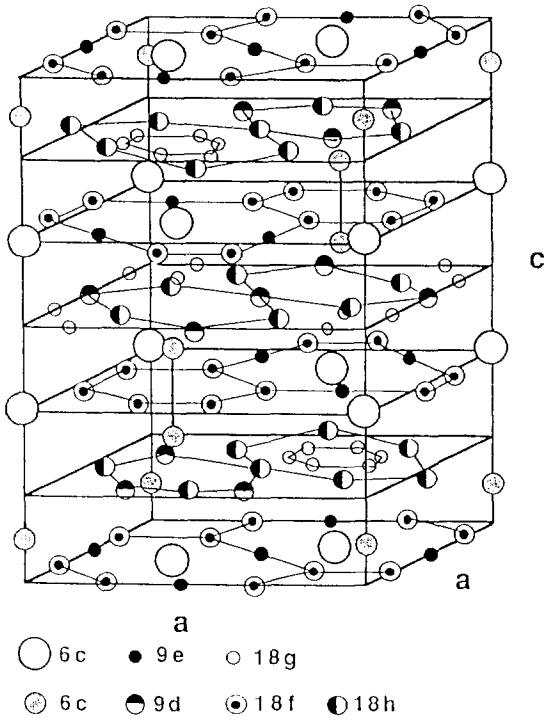

Figure 1. The rhombohedral Th_2Zn_{17} structure.

12] we deduce $\varepsilon_0 \approx 2\%$. For the sake of simplicity we will assume that E and ν do not depend on the local interstitial concentration.

The stress and strain tensors σ_{ik} and ε_{ik}, respectively, are obtained from the thermally averaged concentration profile $\langle c(\mathbf{r})\rangle$ by minimizing the elastic energy

$$U = \frac{1}{2} \sum_{ik} \int \sigma_{ik} \, (\varepsilon_{ik} - \varepsilon^{\circ}_{ik}) \, d\mathbf{r} \tag{2}$$

For spherical grains with a spherically symmetric nitrogen concentration profile $\langle c(\mathbf{r})\rangle = c(r)$ the strain components read [2]

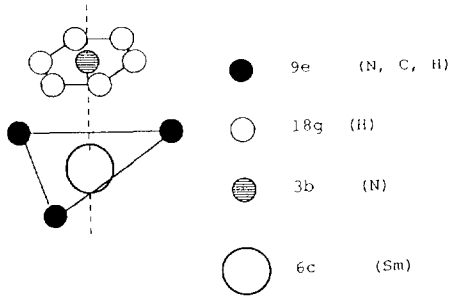

Figure 2. The rare-earth environment in the rhombohedral Th_2Zn_{17} structure [12].

$$\varepsilon_t = \varepsilon_o \left\{ c_{av} + \frac{1 + \nu}{3(1 - \nu)} [c_M(r) - c_{av}] \right\} \tag{3}$$

and

$$\varepsilon_t = \varepsilon_o \left\{ c_{av} + \frac{1 + \nu}{3(1 - \nu)} [3\ c(r) - 2\ c_M(r) - c_{av}] \right\} \tag{4}$$

where

$$c_M(r) = \frac{3}{r^3} \int_0^R c(r)\ r^2 dr \tag{5}$$

Here ε_t is the 'transversal' strain parallel to the particle surface, ε_r describes the radial strain, and $c_{av} = V^{-1} \int \langle c(\mathbf{r}) \rangle\ d\mathbf{r}$ is the average nitrogen concentration.

For flat particles (thin plates) we obtain the comparatively simple results $\varepsilon_t = \varepsilon_o\ c_{av}$ and

$$\varepsilon_z = \varepsilon_o \left\{ c_{av} + \frac{(1 + \nu)}{(1 - \nu)} [c(r) - c_{av}] \right\} \tag{6}$$

where ε_t and ε_z denote the expansions in the transversal x-y and perpendicular z directions, respectively.

Figure 3 shows calculated strain profiles for a parabolic, spherically symmetric concentration profile $\langle c(\mathbf{r}) \rangle = r^2/R^2$. It can be shown that the volume-expansion profiles of thin plates are very similiar to those of spheres, although the respective volume elements dx dy dz and $4\ \pi\ r^2\ dr$ lead to quantitative differences.

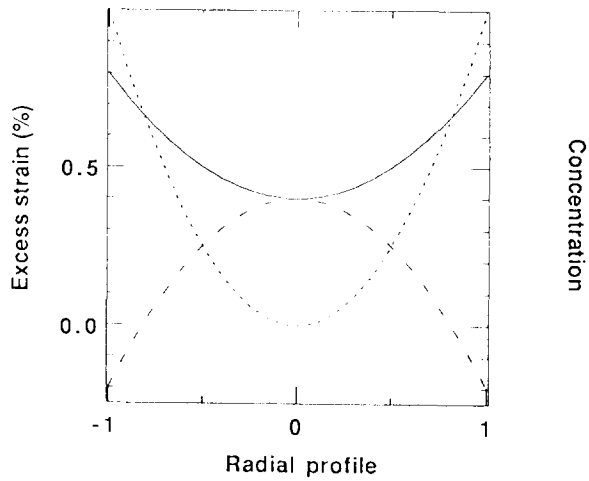

Figure 3. Excess strain in spheres, caused by smooth nitrogen profiles: (dotted line) concentration profile, (solid line) radial excess strain $\varepsilon_r(r) \cdot c(r)\ \varepsilon_o$, and (dashed line) transversal excess strain $\varepsilon_t(r) \cdot c(r)\ \varepsilon_o$.

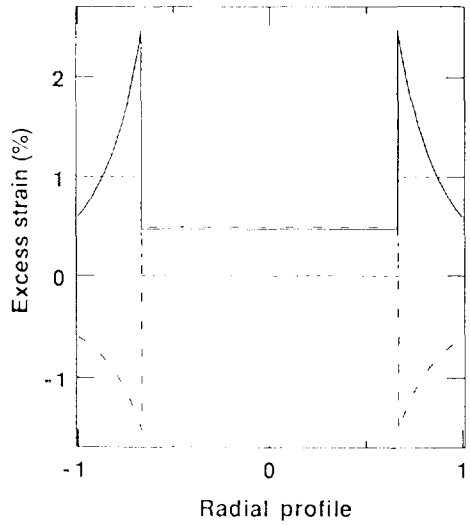

Figure 4. Excess strain in spheres, caused by step-like nitrogen profiles: (dotted line) concentration profile, (solid line) radial excess strain $\varepsilon_r(r) - c(r)\,\varepsilon_o$, and (dashed line) transversal excess strain $\varepsilon_t(r) - c(r)\,\varepsilon_o$.

Figure 4 shows strain and concentration profiles for discontinuous, step-like profiles. The large excess strain shown in Fig. 4 exceeds the range of validity of Hooke's law and is likely to facilitate or even cause microcrack formation. We see that discontinuous nitrogen profiles are accompanied by discontinuous strain and therefore lead to discontinuous magnetic properties. In fact, experiment indicates smoothly varying magnetic properties for N_2-modified powder [2, 12], which is another argument in favour of the solid-solution theory of $Sm_2Fe_{17}N_x$.

Note that gas-phase interstitial modification using ammonia is likely to exhibit a more pronounced tendency towards phase segregation (step-like profiles), since the volume expansion of the 'NH_3' nitrides increases by about 40% if N_2 is replced by NH_3 [6]. In practice, however, it is very difficult to separate this tendency towards phase segregation from the just mentioned lattice disproportionation.

Stress and Strain in Multilayered Nitrides and Hydrides

It is known, for instance from the analysis of NbH_x/TaH_y superlattices [28], that the elastic behaviour of multilayers depends on whether the modification reaction is exothermic or endothermic. Simply speaking, the interstitial atoms enter the regions of the composite for which the reaction is exothermic, while the un-modified regions try to remain as un-expanded as possible. To calculate stress and strain we have to minimize the elastic energy of the multilayer with respect to all freely adjustable parameters.

$Sm_2Fe_{17}N_{3-\delta}$/FeCo Multilayers

In an artificial multilayer $\varepsilon_{xx} = \varepsilon_{yy} = 0$ everywhere, since the substrat acts as a rigid constraint in x and y directions. Compared to Sm_2Fe_{17} particles with free surfaces, the nitrogenation of constrained Sm_2Fe_{17} layers is energetically less favourable: we can think of constrained $Sm_2Fe_{17}N_3$ layers as nitrided free layers which are subsequently compressed in x and y directions. The calculation is straightforward and yields

$$\varepsilon_{zz}(Sm_2Fe_{17}N_x) = \frac{x}{3}\,\frac{(1+\nu)}{(1-\nu)}\,\varepsilon_o \tag{7}$$

and the energy difference

$$\Delta U = \left(\frac{x}{3}\right)^2 V\,\frac{E}{(1-\nu)}\,\varepsilon_o^2 \tag{8}$$

Taking E = 150 GPa, ν = 1/3, V = 87 Å^3 per 9e site, and x = 3 we obtain ΔU = 4.7 kJ/mole. This value is small compared to the net reaction energy U_o = - 57 kJ/mole [2, 7] so that a layer-by-layer nitrogenation of should remain energetically favourable.

6:13:1 Hydrides

Fig. 5 shows the tetragonal $Nd_6Fe_{13}Si$ structure [25]. The unit cell consists of alternating iron-rich and rare-earth rich slabs, with volume fractions f_R and f_{Fe}, respectively. The nominal composition of the hydrides is $R_6Fe_{13}XH_y$ (R = Pr, Nd, ... ; X = Cu, Sb, Bi, ...) where the hydrogen content ranges from y = 13 to y = 20 [25]. The lattice expansion upon hydrogenation is highly anisotropic: the expansion $\Delta a/a \approx 1\%$ in the a-b plane is much smaller than that in the crystallographic c direction ($\Delta c/c$ = 8-13%, depending on the constituent X).

Let us make the physicaly reasonable assumption (cf. [25]) that the hydrogen is concentrated in the rare-earth slabs, i.e. $\varepsilon_o(R) = \varepsilon_R$ and $\varepsilon_o(Fe) = 0$. There are three freely adjustable parameters with respect to which the elastic energy has to be minimized: ε_{xx}, $\varepsilon_{zz}(R)$, and $\varepsilon_{zz}(Fe)$. For $\nu_R = \nu_{Fe}$ the results are

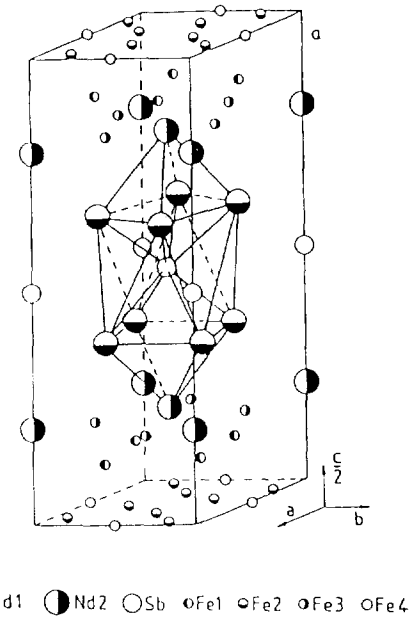

Figure 5. The tetragonal $Nd_6Fe_{13}Si$ structure [25].

$$\varepsilon_{xx} = \frac{f_R E_R}{f_R E_R + f_{Fe} E_{Fe}} \varepsilon_R \tag{9}$$

$$\varepsilon_{zz}(R) = \frac{1 + \nu}{1 - \nu} \varepsilon_R - \frac{2\nu}{1 - \nu} \varepsilon_{xx} \tag{10}$$

and

$$\varepsilon_{zz}(Fe) = - \frac{2\nu}{1 - \nu} \varepsilon_{xx} \tag{11}$$

Taking $f_R = 0.6$, $f_{Fe} = 0.4$, $E_{Fe} = 215$ GPa, $E_R = E(La) = 39$ GPa, $\nu = 1/3$ we obtain $\Delta a/a = 1.7\%$ and $\Delta c/c = 7.9\%$, which is in fair agreement with the experimental values.

Conclusions

Hooke's law for isotropic media is a semiquantitative tool to investigate the elastic behaviour of inhomogeneously modified intermetallic nitrides and hydrides. An exception is stress in discontinuously nitrided grains which exceeds the range of applicability of Hooke's law and is likely to cause microcracks. However, discontinuous concentration profiles in N_2-produced $Sm_2Fe_{17}N_x$ grains would lead to discontinuous stress and strain, anisotropy, and Curie-temperature profiles, which is not observed.

The large c-axis expansion upon hydrogenation of 6:13:1 hydrides originates from the location of the hydrogen atoms in the rare-earth slabs. The situation in these materials is similiar to that of artificial multilayers and thin films, where steric constraints modify the lattice expansion. Calculation yields the prediction that layer-by-layer nitrogenation of hypothetical high-performance $Sm_2Fe_{17}N_3$/FeCo multilayers is possible but energetically less favourable than bulk nitrogenation.

Acknowledgements

The author is grateful to J. M. D. Coey and A. Leithe-Jasper for stimulating discussions. This work forms part of the Concerted European Action on Magnetism and the BRITE/EURAM program of the European Commision.

References

1. J. M. D. Coey and H. Sun, J. Magn. Magn. Mater. **87**, L251 (1990).
2. R. Skomski and J. M. D. Coey, J. Appl. Phys. **73**, 7602 (1993).
3. J. M. D. Coey, Physica Scripta **T39**, 21 (1991).
4. R. Skomski and J. M. D. Coey, J. Mater. Eng. Perf. **2**, 241 (1993).
5. S. S. Jaswal, W. B. Yelon, G. C. Hadjipanayis, Y. Z. Wang, and D. J. Sellmyer, Phys. Rev. Lett. **67**, 644 (1991).
6. R. Skomski, S. Brennan, and J. M. D. Coey, phys. stat. sol. (a) **139**, K11 (1993).
7. J. M. D. Coey, R. Skomski, and S. Wirth, IEEE Trans. Magn. **28**, 2332 (1992).
8. Q.-N. Qi, H. Sun, R. Skomski, and J. M. D. Coey, Phys. Rev. B **45**, 12278 (1992).
9. M. Fähnle and T. Beuerle, phys. stat. sol. (b) **177**, K95 (1993).
10. R. Skomski, M. D. Kuz'min, and J. M. D. Coey, J. Appl. Phys. **73**, 6934 (1993).

11. O. Isnard, S. Miraglia, J. L. Soubeyroux, J. Pannetier, and D. Fruchart, Phys. Rev. B **45**, 2920 (1992).
12. R. Skomski, S. Brennan, and S. Wirth, in: *Interstitial Intermetallic Alloys*, Eds.: F. Grandjean, G. J. Long, and K. H. J. Buschow, Kluwer, Dordrecht 1995, p. 371.
13. R. Skomski, C. Murray, S. Brennan, and J. M. D. Coey, J. Appl. Phys. **73**, 6940 (1993).
14. K. H. J. Buschow, Rep. Prog. Phys. **54**, 1123 (1991).
15. J. M. Cadogan and J. M. D. Coey, Appl. Phys. Lett. **48**, 442 (1986).
16. X.-Zh. Wang, K. Donelly, J. M. D. Coey, B. Chevalier, J. Etourneau, and T. Berlureau, J. Mater. Sci. **23**, 329 (1988).
17. J. H. N. van Vucht, F. A. Kuipers, and H. C. A. M. Bruning, Phillips Res. Repts. **25**, 133 (1970).
18. H. Wagner and H. Horner, Adv. Phys. **23**, 587 (1974).
19. H. Wagner, in: *Hydrogen in Metals I*, Eds. G. Alefeld and J. Völkl, Springer, Berlin 1978, p. 5.
20. V. Alefeld, phys. stat. sol. **32**, 67 (1969).
21. R. Skomski, K.-H. Müller, P. A. P. Wendhausen, and J. M. D. Coey, J. Appl. Phys. **73**, 6047 (1993).
22. R. Skomski and J. M. D. Coey, Phys. Rev. B **48** (1993) 15812.
23. R. Skomski and J. M. D. Coey, IEEE Trans. Magn. **29**, 2860 (1993).
24. J. M. D. Coey and R. Skomski, Physica Scripta **T49**, 315 (1993).
25. J. M. D. Coey, Q.-N. Qi, K. G. Knoch, A. Leithe-Jasper, and P. Rogl, J. Magn. Magn. Mater. **129**, 87 (1994).
26. J. M. Yeomans, *Statistical Mechanics of Phase Transitions*, Clarendon, Oxford 1992.
27. K. G. Wilson, Rev. Mod. Phys. **55**, 583 (1983).
28. P. F. Miceli, H. Zabel, and J. E. Cunningham, Phys. Rev. Lett. **54**, 917 (1985).